

EFFECT OF AZIMUTHAL EXCITATION IN THE NOZZLE EXIT ON STRUCTURES FORMED IN SUBMERGED JETS

Václav Tesař, Václav Něnička, Jiří Šonský, Libor Kukačka, Miroslav Pavelka
Institute of Thermomechanics ASCR v.v.i., Prague

ABSTRACT

Helical structures, due to their chirality property, seem to occupy a special position in fluid mechanics. The paper describes the experimental rig built and the first experience obtained in the course of a project aimed at elucidation of what seems to be these structures capability of self-organization. In the experiment, the structures are generated in the mixing layer of an air jet excited by azimuthal acoustic forcing in the nozzle exit. They are visualised by scattering of "laser knife" light on smoke particles added to the air. Video image data taken were processed by correlation methods to identify the structures and their development.

1. INTRODUCTION

Only relatively recently, some surprising properties were found and recognised of vortical structures in fluid flows having helical character. There are hopes – not unsubstantiated – that their study may have fundamental importance for understanding turbulence, which means understanding fluid mechanics in general because most fluid flows an engineer meets are turbulent flows, at present far from being fully understood. These investigations may also provide cues towards understanding and perhaps in future some control of catastrophic environmental phenomena.

The new aspects of helical instabilities were first discovered in planetary atmospheric flows. The key factor is their extraordinary spectral transport. Large atmospheric phenomena like hurricanes, typhoons, and tornadoes first emerge at small scales and grow, increasing their total energy. Obviously, energies of interacting initial small helical structures are transported towards large size and hence to small wavenumbers [1]. This is the very opposite to the standard direction of spectral transport in turbulence. In the turbulence, deformation of smaller-scale eddies extracts energy from the larger scales in a cascade towards small scales, finally to the size - and Reynolds numbers – so small that the energy is effectively dissipated by turbulence. This course of events apparently does not apply to the helical instability structures; instead of the transport towards dissipation, the energy is transferred towards the large size finally reaching the level of catastrophic dimensions. Starr [2] has shown that this inversion of the spectral transport may lead to effects interpreted as paradoxical negative viscosity.

The capability to unite and form more complex organised structures was recently recognised as being, in general, associated with *chirality* – the left- or right-handedness. Indeed, many examples of self-organisation may be demonstrated to exhibit the chiral character of the units of which they are composed. Recent analysis [1] has shown that this important capability of chiral entities is due to their fundamental thermodynamic non-equilibrium. Of course, the helical instabilities in fluid flows also possess chirality.

These strange facts led to the current project aimed at obtaining more information about helical structures in fluid flows. At present, the research is in its early stage and just gaining the first experience. The aim is primarily to investigate the mechanism of the paradoxical spectral transfer. It is likely to stem from the processes taking place during the interactions between two (or more) smaller structures. This is why this project's activity focuses on generation of two initially independent helical structures and observation of what happens when they meet and interact. Because of the phenomena of interest buried in stochastic turbulence, advanced methods of data processing have to be developed to identify and follow the structures.

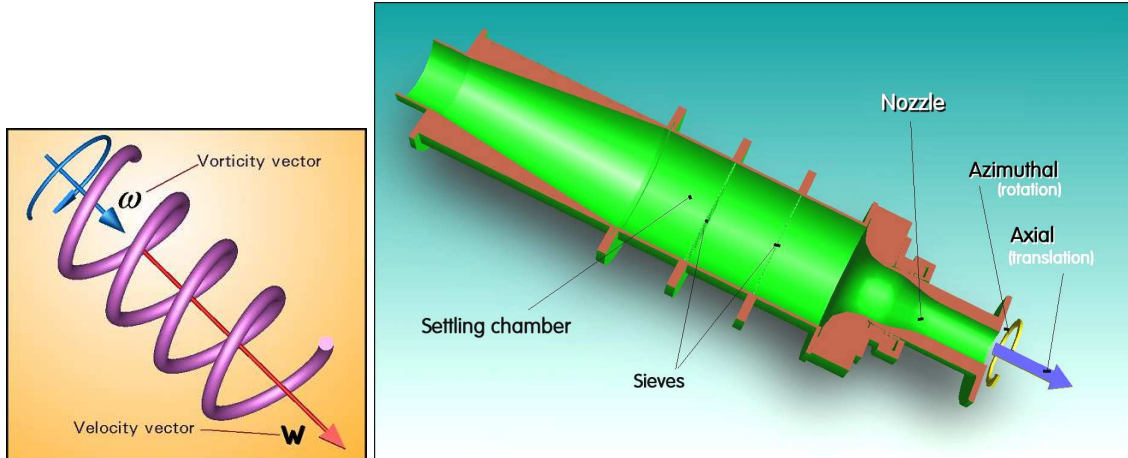


Fig. 1 (Left) A helical object is generated by superposition of translational and rotational motion. The cleanest helix shape is, of course, obtained – as here - when the velocity and vorticity vector directions coincide. This is, in general, an extraordinary situation and most helical objects have the two vectors divergent (and perhaps contain only a part of the loop) so that the helicity may be actually not easy to recognise.

Fig. 2 (Right) The easiest way how to superimpose translational fluid flow with collinear-vector rotation is to apply azimuthal excitation on a nozzle flow. This picture shows the actual 40 mm exit dia nozzle and settling chamber used in the present experiments. The double-contraction shape of the nozzle contour resulted from use of an existing earlier device with quadrant-shaped exit of larger diameter, adapted by insertion of the new, smaller exit.

2. FIRST ATTEMPTS

The easiest way how to generate a helical object is to superimpose rotation on a translatory motion. The generated object will be particularly well shaped if the direction of the translation is collinear with the rotation axis, Fig. 1. As the axially oriented parallel flow component the present project uses submerged jet flows, generated by fluid issuing from a nozzle, Fig. 2. The fluid is air issuing into stagnant surrounding atmospheric air as a submerged jet. The azimuthal motion component should appear spontaneously in the shear layer surrounding the core of the

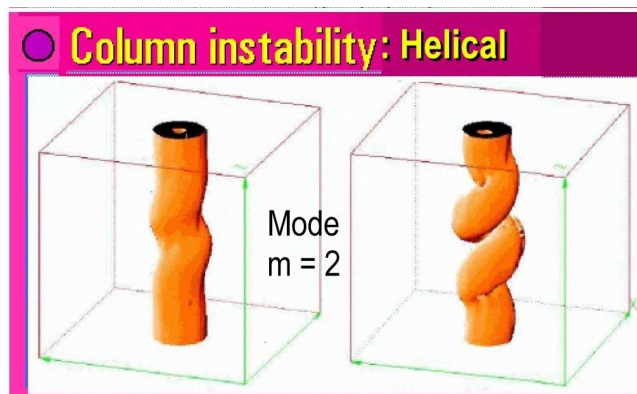
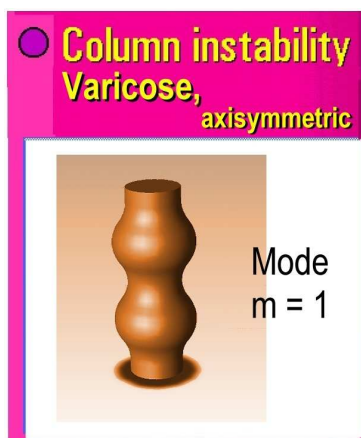


Fig. 3 (Left) Nomenclature taken over from the theory of mechanical vibrations: cylindrical columns can vibrate in infinitely many modes $m = 1, 2, 3, \dots$, of which most important (for energetic reasons) are a few lowest modes. The lowest at all is the varicose, axial motion $m = 1$.

Fig. 4 (Right) The next mode $m = 2$ is the one of importance in the present context. Jets – and in particular turbulent jets (the aim is to study *turbulent* spectral transport) hardly ever retain their coherence for sufficiently long downstream distance to exhibit such clearly discernible motions.



Fig. 5 (Left) Early experiments performed at the University of Sheffield (Tesař, Zimmerman, Regunath [8]) - visualisations of smoke-laden air jet by means of the laser light-sheet "knife". This picture demonstrates spontaneous formation of helical structures in the jet mixing layer.

Fig. 6 (Right) Unfortunately, under nominally identical conditions $Re = 10\ 209$ and no excitation, the vortices sometimes were (seemingly without any apparent reason) formed in the varicose mode $m = 1$.

jet. It really does appear, but the appearance is stochastic and this causes problems associated with phase uncertainty and non-reproducibility.

Moreover, the helical structures are not the only ones that can appear. Early attempts presented at Figs. 5 and 6 have shown [8] that under nominally identical conditions the structures in the jet may be of the unwelcome $m = 1$ varicose mode character instead of the expected helical $m = 2$ ones.

The solution is in triggering the appearance of the structures by periodic excitation of the jet. The excitation power need not be high, because the instability would itself lead to the formation of the structures; the task is just to trigger the formation at the desirable instants of time. Of course, the usual method of jet excitation with the single upstream actuator, Fig. 7, is

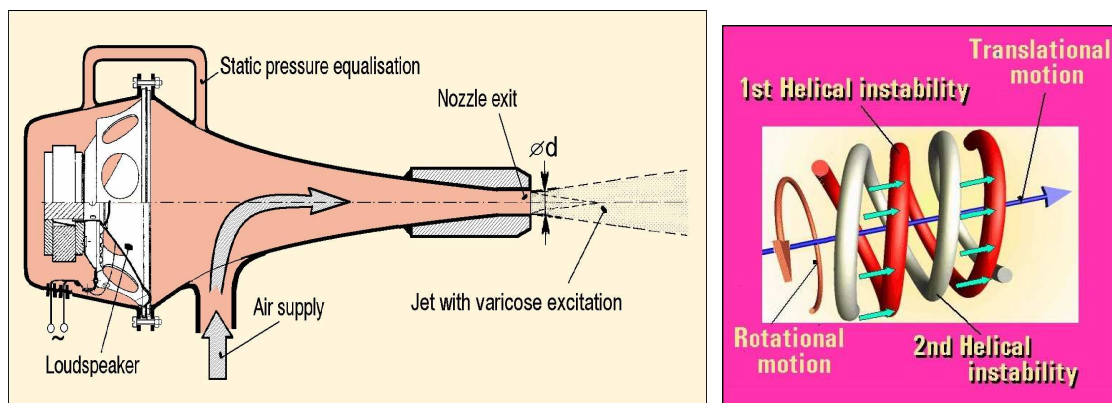


Fig. 7 (Left) A typical case of jet excitation by a loudspeaker located in the settling chamber upstream from the nozzle – in this case as used in [11]. Obviously, this way of excitation would trigger the unwelcome varicose mode.

Fig. 8 (Right) The idea on which is based the proposed use of the experimental rig for studies of the interaction between two intertwined helical instabilities. The arrows show their mutual approaching before the interaction takes place. The instability structures are triggered by the azimuthal excitation acting simultaneously on two locations on the nozzle exit circumference – the locations shifted mutually by 180 deg.

not an acceptable solution as it would preferably trigger the $m = 1$ varicose mode. The excitation needed has to be an azimuthal wave – Fig. 2. If it is desirable to use the electrodynamic actuators (in the form of commercially available loudspeakers), a more complex layout [8] is required.

It should be mentioned that both varicose and helical periodical motion modes can actually appear in two distinct forms. One of them is the column form, with the whole jet periodically deformed as if it were an elastic column. The other one is the mixing layer form, with the structures appearing, like those in Figs. 5 and 6, in the shear layer surrounding the jet core. The problem with the mixing layer is its rather fast development with the increasing streamwise distance from the nozzle. It does not last beyond the distance of approximately ~ 5 nozzle diameters and this also limits the existence of the vortical structures. The fast growth complicates the behaviour of the structures — in particular, their size has to grow in accordance with the layer thickness growth. In principle, from this point of view the columnar form should be perhaps more amenable to investigations – but its size (diameter) also does not remain constant, grows as well, and it is usually strongly disturbed by the present stochastic turbulence. It is pointless to concentrate on laminar jets (which are more regular and their lateral dimensions do not grow so fast) if the overall aim is to study the spectral transport in turbulence. There is also the size problem to be solved in designing the rig: generation of laminar jets would call for small nozzle size, of the order of a few millimetres. At such small scale, it would be very difficult to make the optical measurements, which are the only suitable approach if the jet is not to be disturbed by any invasive detection method. Light sheet thicknesses of the available “laser knife” devices are usually of the order of millimetre (at the suitably large distance of the laser optics from the nozzle) so that it would be useless in the laminar jet of a comparable thickness (this, after all, is the well-known problem that has led to micro-PIV as a special branch).

3. EXPERIMENTAL SETUP

The above considerations have led to the decision to study the jets that are turbulent - or in transition into turbulence, at Reynolds numbers of the order $1 \cdot 10^3 - 10 \cdot 10^3$. A suitable nozzle size $d = 40$ mm was chosen as being large enough for convenient flow visualisation imaging and small enough for convenient operation of scattering particle generators. The rig operates with air, supplied by a blower driven by a precise frequency changer Hitachi L200-004NFEF2

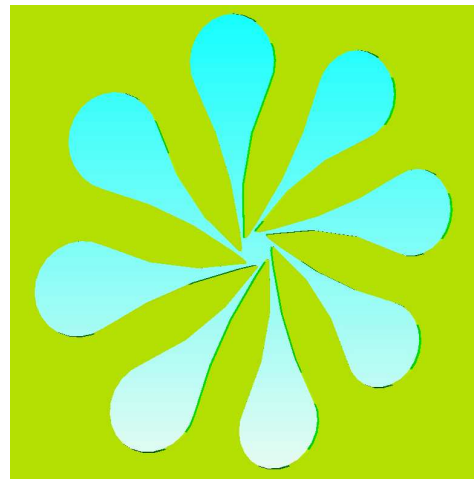
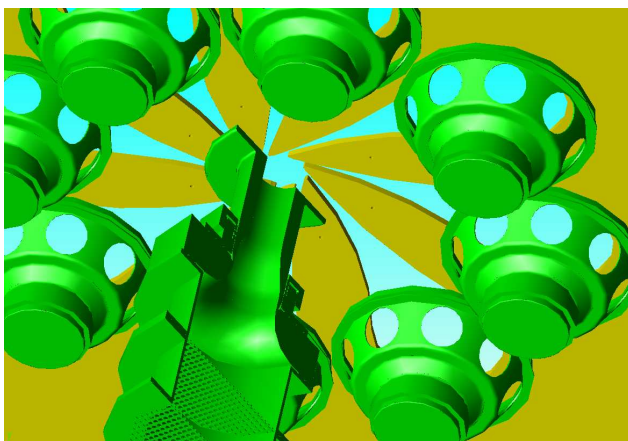


Fig. 9 (Left) View from below on the nozzle (shown sectioned) and the system of circumferentially positioned loudspeakers used to generate the desirable azimuthal excitation. The top cover plate as well as two other plates (including the one that actually holds the loudspeakers) are here removed..

Fig. 10 (Right) The "Catherine wheel" cutouts in the plate serve as acoustic waveguides transferring the output of the loudspeakers to the nozzle exit. Since only one sense of the azimuthal waves orbiting is planned, the waveguide exits are inclined tangentially.

permitting an exact speed adjustment and keeping of the selected air flow rate. Performance and characteristics of the blower were investigated in a separate study, summarised in [4]. The scattering particles are currently glycerine particles produced by evaporation and condensation upstream from the blower entrance – with plans of using water mist in the future instead of the glycerine to obtain conditions nearer to the atmospheric phenomena. The rig was actually designed for future adaptation to generate small tornado models as described in report [3]. The nozzle was found to produce reasonably flat velocity profile in its exit; its aerodynamic properties were also already previously studied in detail, as reported in [5]. The settling chamber upstream from the nozzle, with two flow-settling sieves, was taken over from an earlier experimental rig.

The most interesting part of the rig is the actuator for generating the azimuthal excitation of the jet mixing layer. In principle, based on the analogy with three-phase electric motor, the rotating acoustic field may be generated by three transducers fed by the three-phase current, positioned at 120 deg around the nozzle exit. However, the operating frequency has to be adjustable and adjusting three phases is inconveniently complicated. A better solution is using four transducers positioned at 90 deg: the spatial approximation to the ideal azimuthal progress of the generated wave is better and it is possible to change the frequency in only two channels – the remaining two phases are obtained by simply interchanging the soldering points (which shifts the motion in an electrodynamic drive by 180 deg in phase). The idea of investigating the interaction of two helical structures (Fig. 8) complicated the design further. What is needed are two azimuthal waves chasing one another on the opposite sides of the jet core. This requires twice as more drives: 8 electro/acoustical transducers. Again, standard commercially available

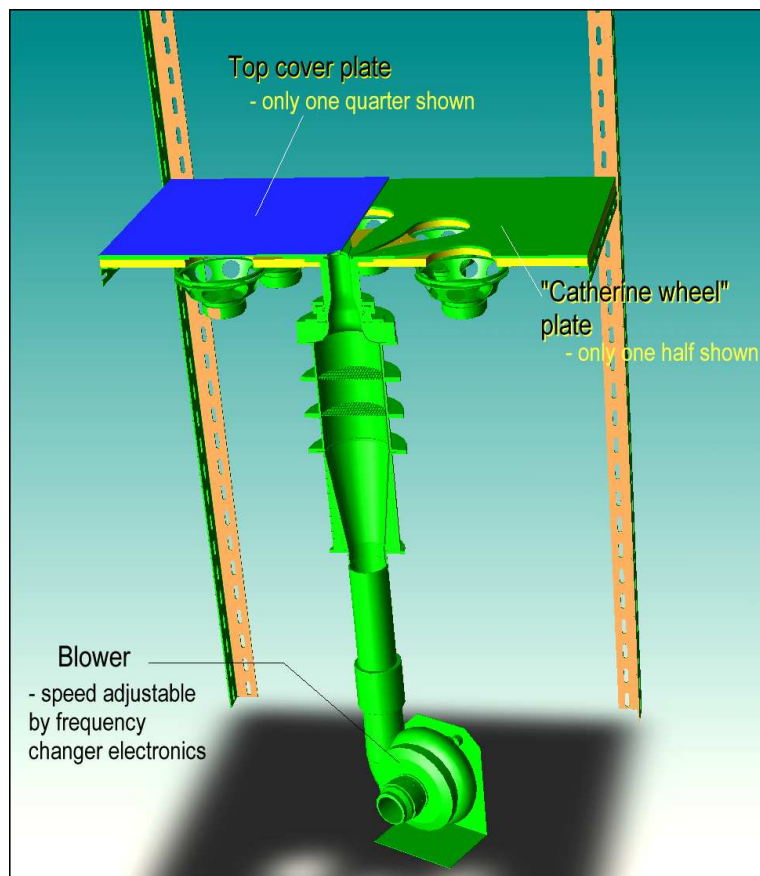


Fig. 11 The essential part of the airflow generation rig, shown partly sectioned. Note the positions of the loudspeakers, corresponding to the previous Fig. 9, and the “Catherine wheel” plate from Fig. 10 delivering the air displaced by the loudspeakers towards the central nozzle exit.

loudspeakers are used as the drives – Figs. 9 and 11. The 8 drives cause no problem on the electric side compared with the 4-drives version for a single helical structure: the two channels of are simply connected also to the drives located on the opposite side of the nozzle. The loudspeakers are low-frequency woofers ARN-165-01/4 supplied by TVM Acoustic Ltd., of nominal power 100 W specified by the manufacturer (– authors’ unpleasant past experience has shown that the nominal value is not applicable for continuous operation with a harmonic signal).

The smoke was introduced far upstream - in front of the entrance into the blower (Fig. 12) thus ensuring homogeneous mixing with the air. The one used in the experiments as they are described below was a borrowed DANTEC Dynamics FOG 2004 fog generator, generating oil droplets guaranteed to be of $\sim 3 \mu\text{m}$ diameter.

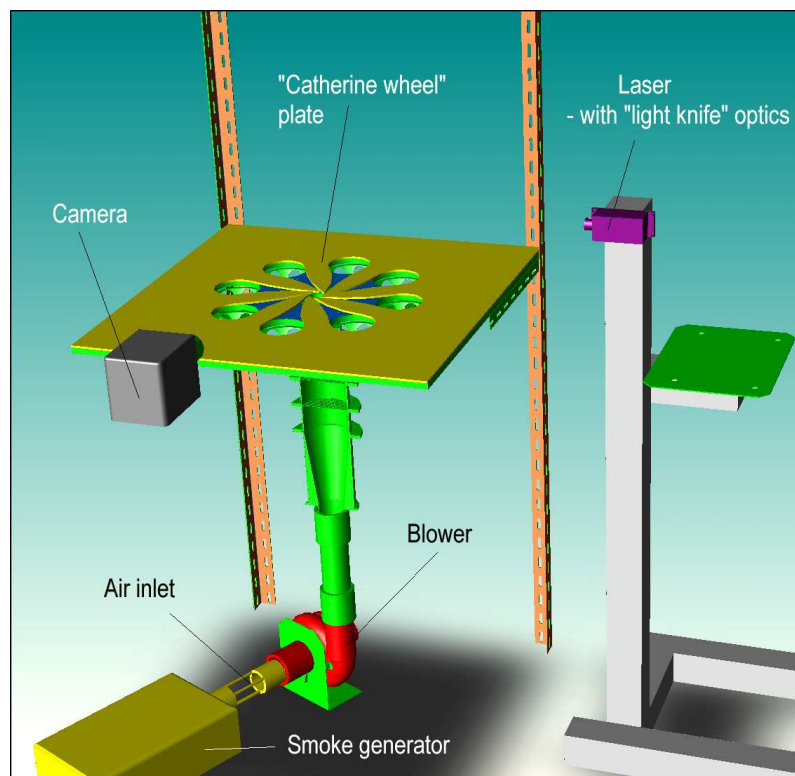


Fig. 12 Another view of the experimental setup, showing the position of the camera and the laser. The surface around the nozzle exit is actually covered with the top cover plate, the one only one quarter of which is shown in blue colour in previous Fig. 11 – this plate closes on top the waveguides leading towards the central nozzle exit.

The laser used for the “laser light knife” was diode pumped solid state green light (wavelength 532 nm) Nd:YAG laser DPGL-2200L-45 supplied by Shanghai Uniwave Technology Ltd. Its maximum output power is 200 mW; the power is continuously adjustable and during the experiment the values were usually lower than this maximum. The laser was delivered by the supplier with cylindrical optic generating the light sheet (Fig. 13) with fan angle 45° and guaranteed width $< 5 \text{ mm}$ at 5 m distance – the distance actually used was, of course, much shorter $\sim 700 \text{ mm}$, so that the sheet thickness was $\sim 0.7 \text{ mm}$.

The camera used in the course of the present experiments was Vision Research Phantom v7.3 continuously recording 14-bit mono, SR-CMOS sensors digital camera with 800×600 pixels resolution (standard TV screen format) and top speed of 6 688

frames per second – which was not used in the present case, where the data acquisition speed was 100 frames per second. The images were stored as a video clip containing 1s of camera run, i.e. 100 frames.

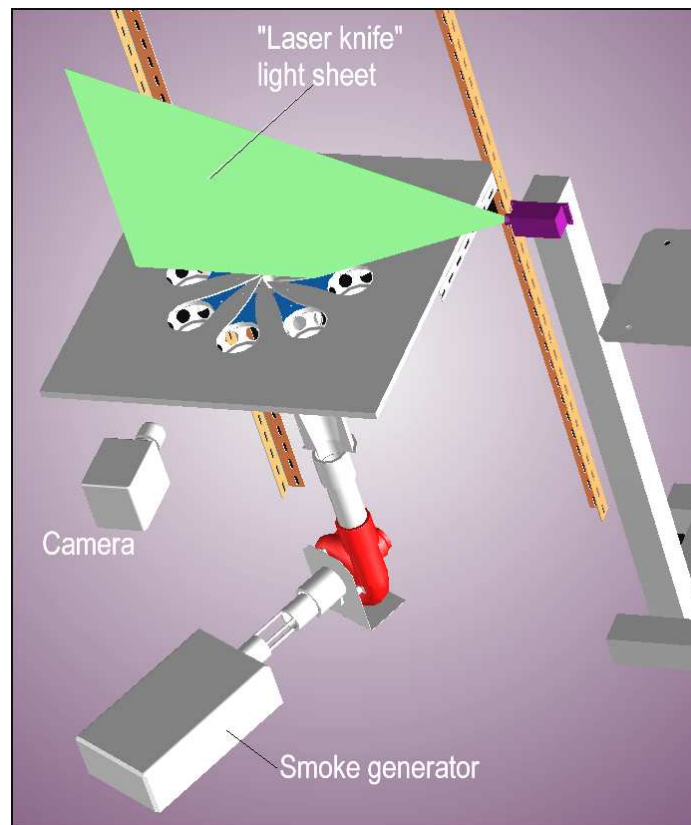


Fig. 13 The camera sees and stores the light scattered from the smoke particles in the plane defined by the “laser knife” light sheet and this way produces an information about the local amount of outer air (not contaminated by smoke) entrained into the smoke-laden jet.

4. IMAGE DATA PROCESSING

The fundamental idea is identification of spatial time-varying structures from image data obtained by visualisation in a single plane. The method employs the almost-periodic character of the structure dynamic.

The images stored as the output from the camera were 800×600 matrices of values which represented the local intensity of the laser light scattered on the glycerine droplets – roughly proportional to the local droplet density. The entrained external atmospheric air contained no droplets. On the image, it appeared black. The value stored at the corresponding pixel of the camera image was 0. Increasing concentration of the droplets has led to gradual increase of this value. The matrices were processed using MATLAB software.

The idea on which the image data processing was based was the correlation analysis as described in [12] and [13]. The processing procedure consisted of the following steps:

- 1) Downloading the video clip
- 2) Normalising and converting the data value at each pixel into corresponding colour and presenting the image using the `colormap` command. The pictures obtained were mentioned as showing “*absolute intensity*”.

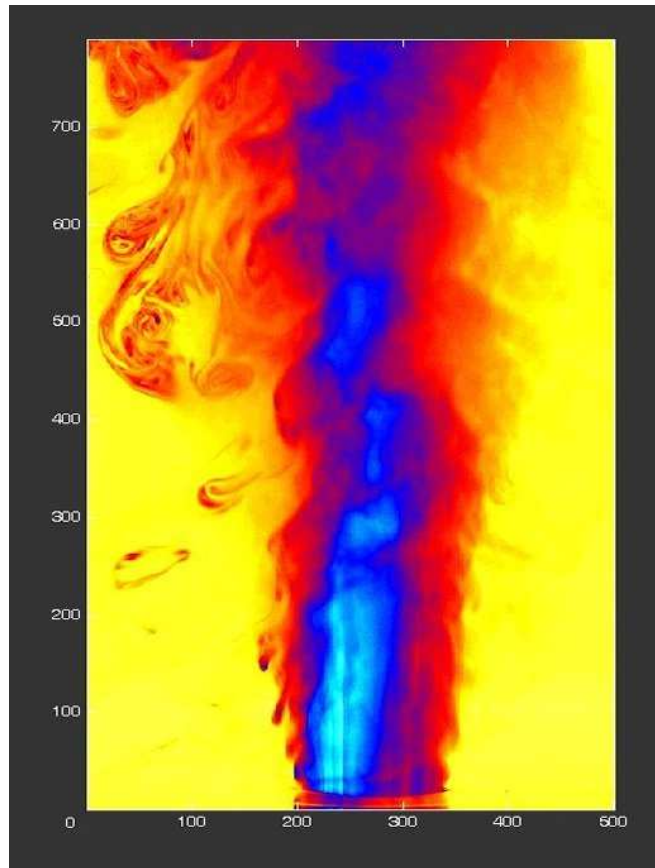


Fig. 14 An example of jet image data. What is presented here is called “*absolute intensity*” picture showing colour coded local intensity of the light scattered from the smoke particles. Jet velocity in the nozzle exit was $w = 0.46$ m/s, excitation frequency $f = 25$ Hz, Reynolds number 1 170, Strouhal number 2.18.

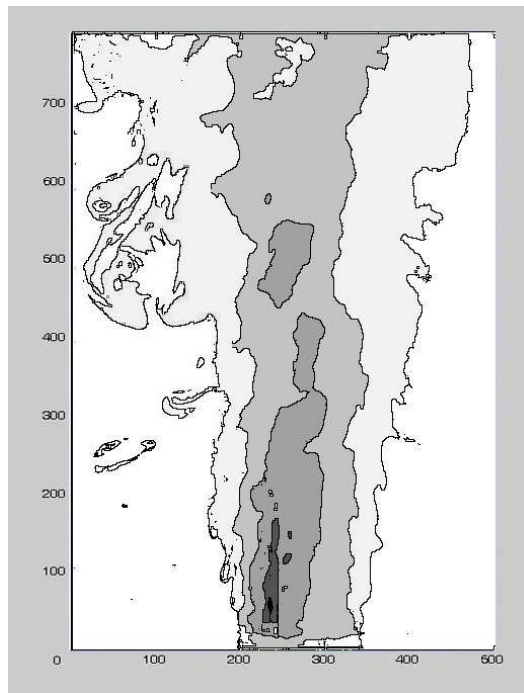


Fig. 15 An example of posterisation of the jet image data. The colour coded picture from Fig. 14 with drastically reduced colour palette – here converted to grey scale – may be useful for identifying structures in the jet.

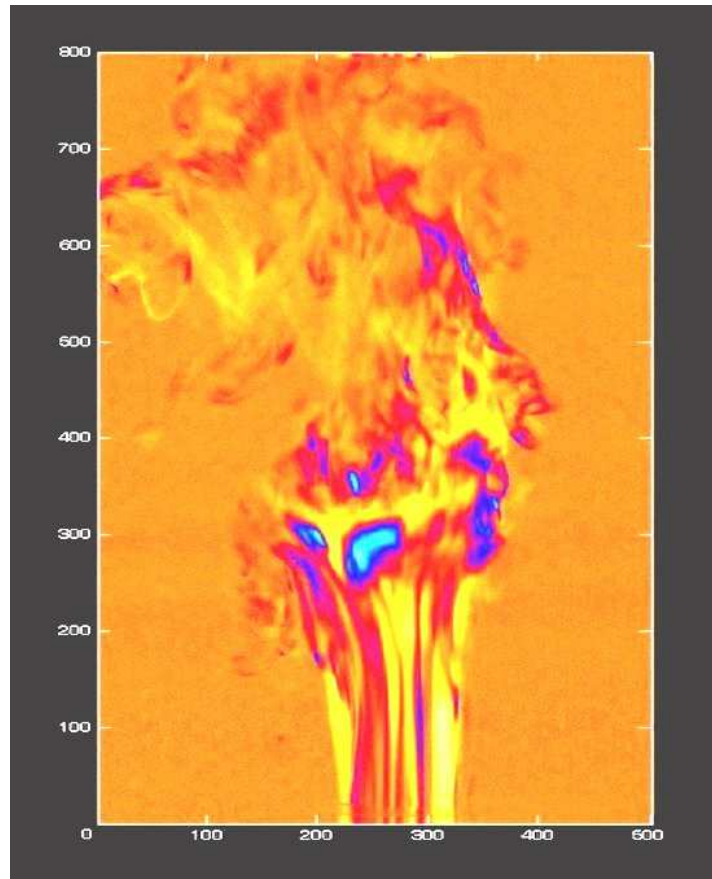


Fig. 16 Relative intensity data for the scattering on smoke particles. The picture was taken at jet velocity in the nozzle exit $w = 2.36$ m/s, excitation frequency $f = 4$ Hz, so that Reynolds number was $Re = 6\ 020$, Strouhal number $Sh = 0.068$. Data from identical position pixels were taken from the set of 3 previous and 3 next frames evaluate the mean. The colour coding of the relative values indicates the magnitude of the local deviations from the local mean value. The instability structure is betrayed by the light blue colour as the location where the flowfield changes most rapidly.

- 3) Visual inspection of the clip and selection a suitable sequence of at least 6 frames showing an interesting or promising feature.
- 4) Computation of the mean value at a particular location in the matrix from the 6 values in the sequence of 6 frames.
- 5) Subtracting the mean value from the value of the sequence. The pictures obtained were mentioned as showing “*relative intensity*”.
- 6) A pixel cluster was chosen in the neighbourhood of the interrogated location to represent a spatial comparison vector. For the frames in the sequence, a correlation is computed for the values of the equally located interrogation points in two frames from the sequence. The pictures obtained this way were referred to as showing “*spatial correlation*”.
- 7) Since the frames in the sequence differ by the equal time step $\Delta t = 1/100$ s, it is possible to compute the correlation between the equally located interrogation points. The pictures obtained this way were referred to as showing “*temporal correlation*”.

The accompanying illustrations present examples of the images obtained by this processing approach. An example of jet image data in the “*absolute intensity*” colour coding is in Fig. 16. The colours shown are actually negatives of the standard MATLAB output. The aim of the

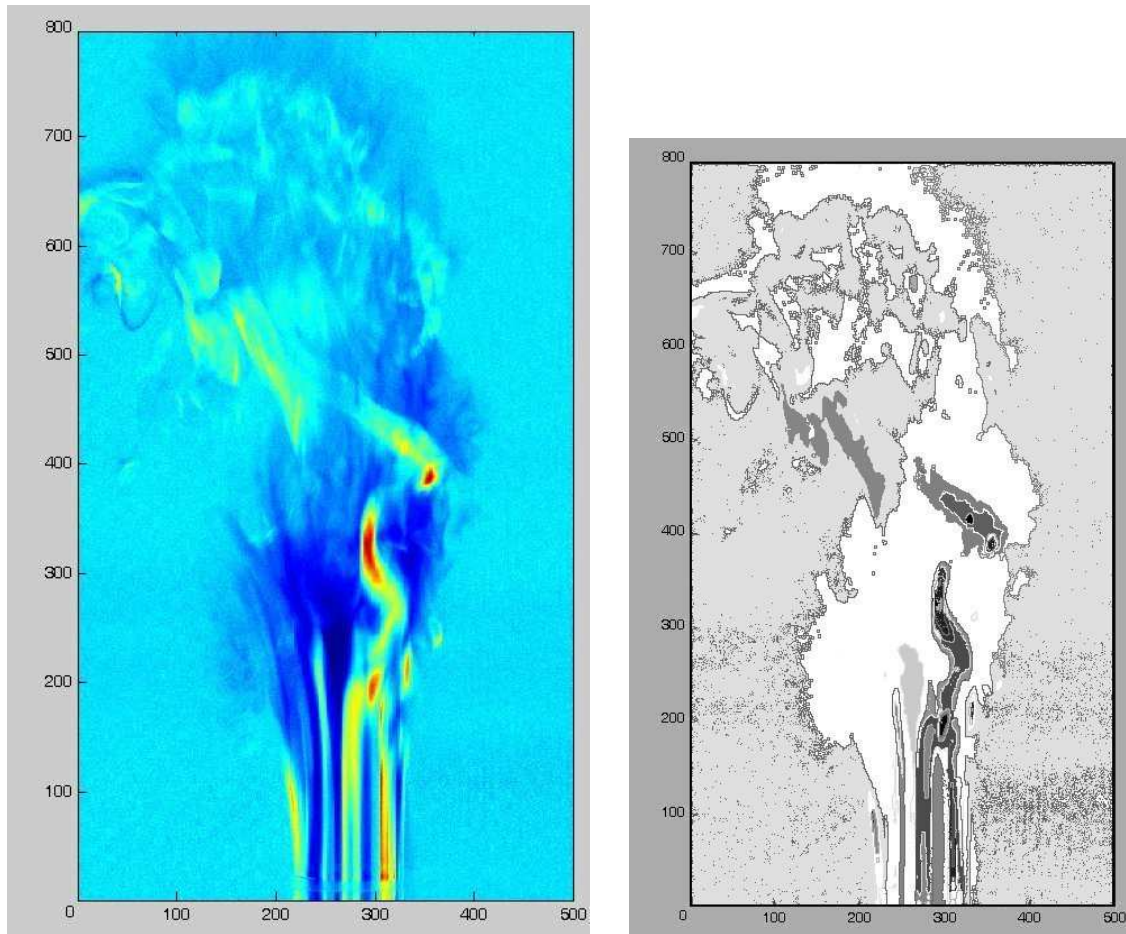


Fig. 17 (Left) Relative intensity data for the scattering on smoke particles. The picture was taken at the same conditions ($Re = 6\ 020$, $Sh = 0.068$) as in the example in Fig. 16 – but for different sequence of the six frames.

Fig. 18 (Right) The image from Fig. 17 shown posterised and converted into the greyscale.

processing being identification of structures – which are betrayed by having comparable and usually high concentration of the scattering particles — it is useful to reduce the colour palette of the pictures. This makes easier visual evaluation of the areas in the frame that may be the “laser knife” sections of the vertical structure. The process of the drastic reducing of the palette is known as “posterisation”- ref. [14]. In Fig. 15 the camera frame from Fig. 14 is shown posterised and converted into greyscale.

An example of the jet image data in the “*relative intensity*” colour coding is in Fig. 16. There seems to be an instability structure indicated by the light blue colour just below the centre of the picture. Obviously, with the very large difference from the mean, in this location the density of the scattering particles varies very rapidly. Another example of the “*relative intensity*” colour coding together with the posterised alternative is in Figs. 17 and 17.

The simple indication of the change by subtraction of the sequence mean may be not a convincing detection criterion in the search for the instability structures. The correlation approach is more sophisticated and probably better. An example of the computed “*spatial correlations*” in Fig. 19 were computed from the “*absolute intensity*” data. The resultant pictures of these type are sometimes referred to as “*absolute spatial correlation*”. The colours

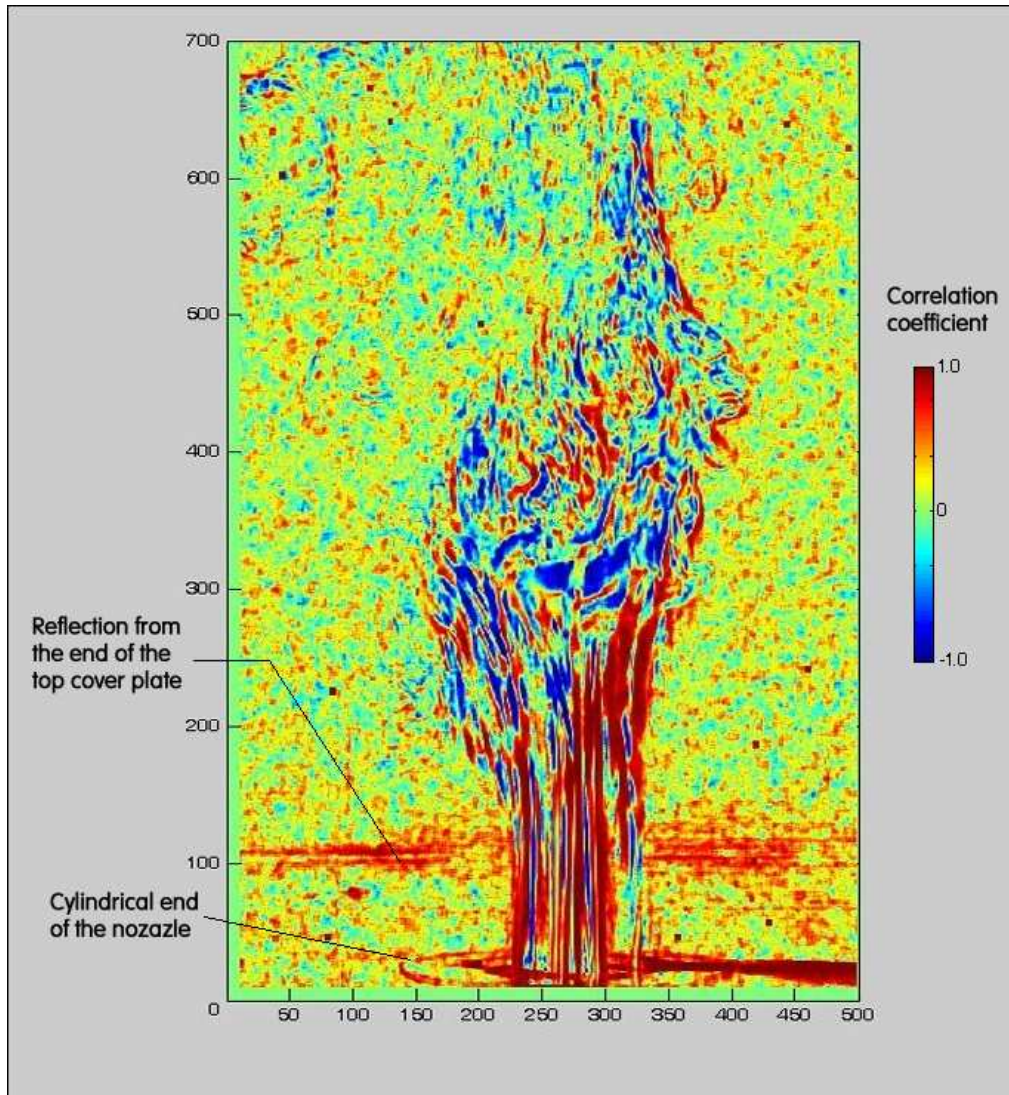


Fig. 19 Spatial change correlation evaluated using the absolute optical density data. Locations coloured red are those where the flow features are steady during the time interval between two frames. Blue coloured areas of large negative correlation coefficient indicate intensive changes in opposite direction between the two correlated vectors. The green colour indicates chaotic behaviour.

in this picture represent the values of the correlation coefficient R , which may assume values between $R = 1$ if the image features do not change in the course of picture taking, and $R = -1$ if the features change and retain the characteristic shape. The cases of $R = 1$ are coloured red in Fig. 19. Among them are two features that actually have nothing in common with the air flow: there is the elliptical shape (actually representing a circular object) surrounding the nozzle exit. This became visible due to light scattering on the outer surface of the nozzle from which the air jet issues. The other feature is the scattering from the far end of the top cover plate (cf. Fig. 11) that incidentally was also captured in the camera picture. Both these objects are stationary and there is no wonder the computation algorithm reveals them in the red colour. More important for the aim of this research are the areas coloured blue. They indicate the structures in the flowfield. Unimportant are the regions in which the green colour indicates correlation coefficient R values near zero – the changes evaluated as the sequence progresses are there chaotic, uncorrelated. This is the situation – as expected – in the regions outside the jet. The

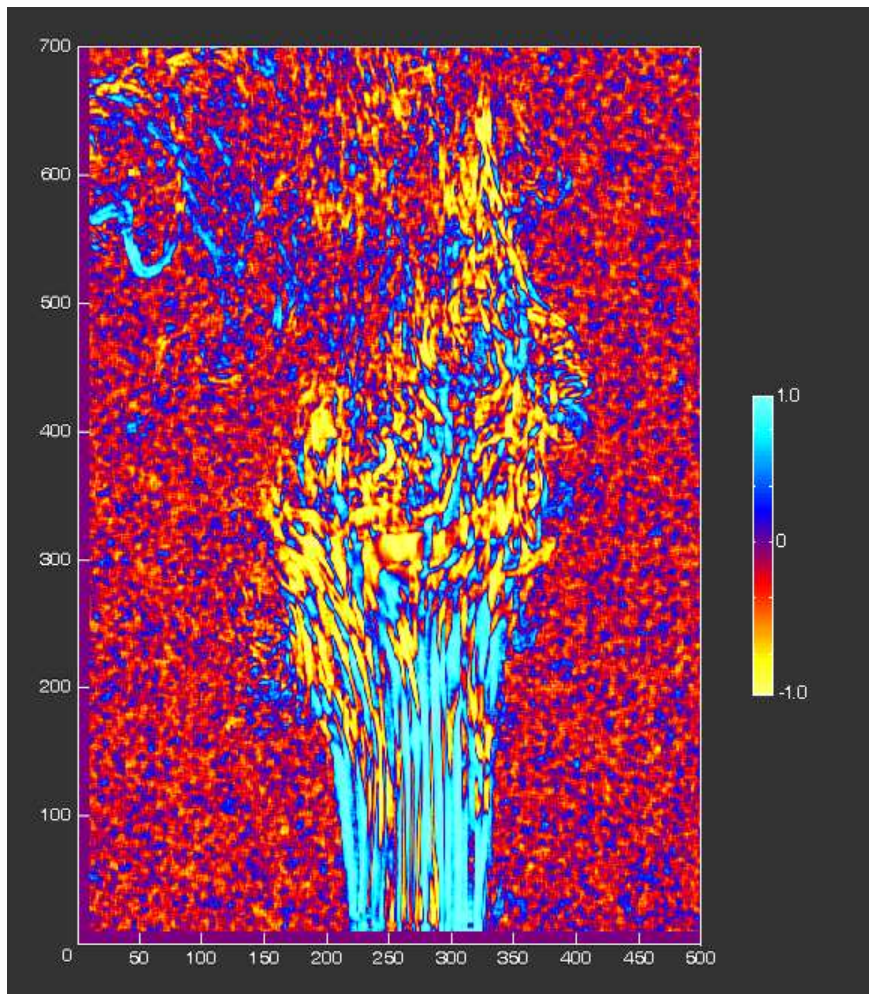


Fig. 20 Spatial change correlation evaluated for the same frame as in Fig. 16 using the relative optical density data presented in that picture. Locations coloured light blue are here those where the flow features do not change relative to the mean values – the flow there is steady. The yellow coloured areas of large negative correlation coefficient indicate intensive changes, relative to the mean, proceeding in the opposite direction. The red colour indicates chaotic behaviour.

speckles, red and blue “dots” in these green areas are of no importance and may be ignored. They are produced by noise in the correlation evaluation – and could be in principle removed by some even more sophisticated image processing.

Another, related approach to processing image data by the correlation method is the so called “*absolute spatial correlation*” – an imprecise description which means that “*spatial correlations*” are computed from the “*relative intensity*” data distribution. An example of such processing is presented in the following Fig. 20. What should be noted when comparing this picture with the previous Fig. 19 is the different usage of the colour coding: here it is the yellow colour that indicates the important areas of large negative correlation coefficient $R \rightarrow -1$. On the other hand, the light blue colour is indicative of the steady features, little or not at all changing relative to the mean of the whole frame sequence. Perhaps it is advisable to note that “steady” here does not mean “stationary”, or “non-moving”. In fact the light blue colour is mainly seen in the region immediately downstream from the nozzle exit, where the flow velocity is actually maximum. The organised character of the flow there is not surprising in

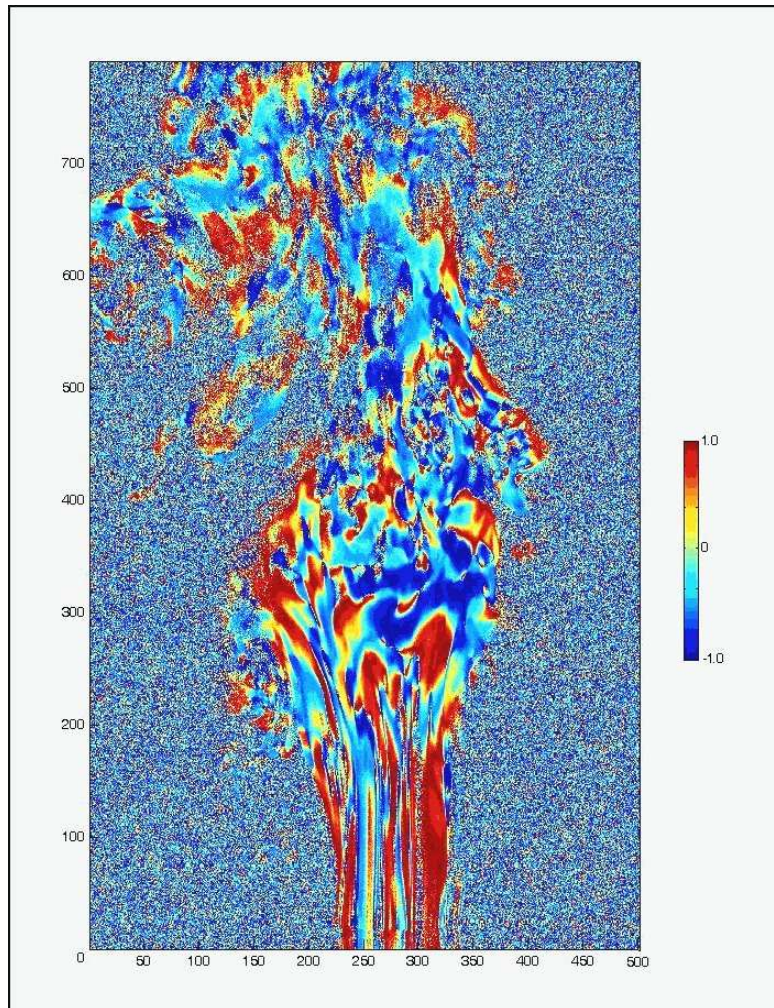


Fig. 21 Temporal changes evaluated from computed correlation, again for the same frame as in Fig. 16. This is yet another way how to detect locations exhibiting a coherence in their changes. For characterisation of temporal changes, 6 temporal neighbour frames were used.

view of the low $Re = 6\ 020$. There is a remarkable change of flow dynamics with the downstream distance from the nozzle exit, obviously the onset of developed turbulence.

Finally, there is also the possibility to compute the correlations in the purely temporal sense – progressing along the sequence of the frames in the video clip. The results of that approach are shown in the last example in Fig. 21. Again, the processed data are those of the same sequence used for evaluation of the other examples presented in Figs. 16 and 20.

The correlation approach used here promises to provide a useful insight into the formation and development of the structures of interest. Admittedly, the examples presented above did not lead to any spectacular detection of the sought helical structures. After all, they were taken in the course of the first experiments in which the main task was to gain experience with this approach. It seems that the azimuthal excitation was too strong and destroyed rather than triggered the formation of helical structures. This is apparent from the fact that at Reynolds numbers comparable or even lower than those at which the un-excited flows (in Fig. 5 and 6) exhibited smooth, low turbulence flow, in the examples presented in the present paragraph all the flows were strongly disturbed.

To sum up, the examples as presented above demonstrate that the correlation approach is a viable alternative for the image data processing to detect instability structures. The appearance

of these structures in the fluid flows and their consequent development may be characterised either by spatial or by temporal negative correlation within a chosen series of frames forming a sequence.

The computed temporal correlations will provide a source of information about the conditions under which the formation of a structure can begin. On the other hand, the spatial correlations will provide an information about the location of the structures.

5. CONCLUSIONS

The authors demonstrated operational readiness of the rig that has been built for investigations of helical instability structures generated in the mixing layer of a submerged axisymmetric jet. An important contribution is the correlation approach to the image data processing. Using the quasi-periodic character of the structures, this approach detects a three-dimensional entity by analysis of temporal development of data acquired by visualisation in a single plane.

Spatial correlations are computed by comparing spatially defined vectors of changes of the locally detected intensity of the scattered light from the smoke particles in the jet. The temporal correlations also follow from the same frame sequence. The difference between them is in the correlation being in the temporal case computed from the changes found between the frames in the sequence.

In the non-synchronised operations run so far, an example of which was provided by the case discussed in the part 4, there are four degrees of freedom in adjusting the conditions:

- nozzle flow rate – that determines the Reynolds number,
- excitation frequency – determining the Strouhal number,
- amplitude of the excitation, and
- camera frame grabbing frequency – which determines the time step, a quantity of importance for computing the temporal correlations.

In addition, there are also auxiliary variables that have to be properly adjusted and the influence of which has to be also learned. It is the proper laser light intensity and the density of the smoke at the output of the smoke generator.

At this stage, the procedure was not yet used to detect the sought structures because the authors were not yet able to adjust these variables properly. The adjustable parameters mentioned above were so far varied in a non-systematic way, mainly to find out what are the essential features of the investigated flow. Proper choice of the variable magnitudes so as to detect and identify a well defined helical structure — and later two mutually interacting structures — is obviously possible, but has to be guided by experience, which is yet to be gained. The authors so far concentrated on demonstrating the capability to perform this type of experiment and to process the resultant image data. It is now practically certain that the experimental rig is a useful tool. Its capabilities will be at a later stage of the project improved by the synchronisation of the frame grabbing by the camera with the excitation signal. The value of the processed images will then be further improved by the phase averaging process.

ACKNOWLEDGMENTS

The authors gratefully acknowledge the financial support by the grant IAA200760705 provided by Grant Agency of the Academy of Sciences of the Czech Republic. Another partial support was also obtained from the grant Nr. 101/07/1499 donated by the Grant Agency of the Czech Republic. Also gratefully acknowledged is the invaluable capability of technician Mr. J. Šafář who set up the experimental rig.

References

- [1] Moiseev S. S., Pungin V. G.: "Analysis of Nonlinear Development of Helical Vortex Instability", Fractals, p. 395, Vol. 10, No. 4, 2002
- [2] Starr V.: "Physics of Negative viscosity Phenomena", McGraw-Hill, New York, 1968
- [3] Tesař V.: "Koncepce experimentálního zařízení pro výzkum proudění se šroubovicovými nestabilitami" (General idea of the experimental rig for investigations of flows with helical instabilities – in Czech), Report Z 1405/07, Institute of Thermomechanics ASCR v.v.i., Prague, Czech Republic
- [4] Tesař V., Kukačka L., Kellnerová R.: "Investigation of Characteristics of a Blower used as an Air Source in an Experimental Rig for Studies of Helical Instabilities in Flowing Fluids", Proc. of Colloquium FLUID DYNAMICS, Institute of Thermomechanics of the Academy of Sciences of the Czech Republic, v. v. i., Prague, ISBN 978-80-87012-07-09, October 2007
- [5] Tesař V., Kellnerová R., Kukačka L., Kordík J.: "Properties of Nozzles – Experimental Verification on the Rig Built for Helical Instability Investigations", Proc. of Conference 'Topical Problems of Fluid Mechanics 2008', p. 113, Institute of Thermomechanics of the Academy of Sciences of the Czech Republic, Prague, February, 2008
- [6] Oberleithner K., Paschenreit O., Wygnanski I.: "Vortex Breakdown in Swirling Free Jets. Part 2. On the Natural and Forced Instabilities", 2nd. Int. Conf. On Jets, Wakes and Separated Flows, September 2008, Berlin, Germany
- [7] Tesař V.: "Time-Mean Helicity Distribution in Turbulent Swirling Jets", Acta Polytechnica – Journal of Advanced Engineering, ISSN 1210-2709, Vol. 45, No. 6, p. 9, 2005
- [8] Tesař V., Zimmerman W.B.J., Regunath G.: "Helical Instability Structures in Swirling Jets", Proc of the 8th Internat. Symp. on Fluid Control, Measurements, and Visualization FLUCOME 2005, Chengdu, China, 2005
- [9] Regunath G., Tesař V., Zimmerman W.B.J., Hewakandamby B.N., Russell N.V.: "Experimental Investigation and Visualization of Helical Structures in a Novel Swirling Jet", Proc. of FEDSM06, ASME Joint U.S. – European Fluids Engineering Summer Meeting, Technical 32-5, Miami, Florida, U. S. A., July 2006
- [10] Regunath G.S., Zimmerman W. B., Tesař V., Hewakandamby B. N.: "Experimental investigation of helicity in turbulent swirling jet using dual-plane dye laser PIV technique", Experiments in Fluids, ISSN 0723-4864, Springer Berlin/Heidelberg, DOI 10.1007/s00348-008-0515-3, Vol. 45, 2008
- [11] Tesař V., Ho C.-L. : "Resonant Structure in an Axially Excited Axisymmetric Jet", Proc of Colloquium "Topical Problems of Fluid Mechanics", ISBN 80-85918-36-6, Publ. by IT AS CR , p. 39, February 1998
- [12] Něnička V., Hlína J., Šonský J., Krejčí L.: "Application of the Correlation Analysis to Identification of Coherent Structures in Free Plasma Flow", Acta Technica CSAV, ISSN 0001-7043, p. 175, Vol.. 48, Nr. 2, 2003.
- [13] Něnička V., Hlína J., Šonský J.: "Diagnostics of Dynamic Phenomena in Thermal Plasma Jets by a CCD camera", IEEE Trans. Plasma Sci.. 33, p. 418, 2005
- [14] Tesař V., Barker J.: "Dominant Vortices in Impinging Jet Flows", Journal of Visualisation, Japan, ISSN 1343-8875, p. 121, Vol.5, No.2, 2002
- [15] Regunath G., Tesař V., Zimmerman W.J.B., Russel N.: "Novel Merging Swirl Burner Design Controlled by Helical Mixing", Paper 0153 – 002, 7th World Congress of Chemical Engineering, Glasgow, 2005.
- [16] Trávníček Z., Kopecký V., Maršík F., Tesař V.: "Bifurcated and Helical Impinging Jet Controlled by Azimuthally Arranged Synthetic Jets", Proc. of HEFAT2007, 5th International Conference on Heat Transfer, Fluid Mechanics and Thermodynamics, Paper TZ1, ISBN:978-1-86854-6435, Sun City, South Africa, July 2007.

